Hindawi
Mathematical Problems in Engineering
Volume 2022, Article ID 1998227, 11 pages
https://doi.org/10.1155/2022/1998227

Research Article

Study on the Influence of Cracks on the Mechanical Performance of Tunnel Lining Structure Based on Fracture Mechanics Theory

Taotao Hu,[1,2] **Xiong Hu**,[1] **Jianxun Chen**,[1] **Chuanwu Wang**,[1] **and Yi Yang**[3]

[1]*School of Highway, Chang'an University, Xi'an 710064, China*
[2]*State Key Laboratory for Strength and Vibration of Mechanical Structures, School of Aerospace Engineering, Xi'an Jiaotong University, Xi'an 710049, China*
[3]*Alxa League Transportation Engineering Quality and Rural Highway Service Center, Alxa League 750306, China*

Correspondence should be addressed to Taotao Hu; tthu@chd.edu.cn and Chuanwu Wang; wangcw17@163.com

Received 9 March 2022; Accepted 9 April 2022; Published 9 May 2022

Academic Editor: Fuqiang Ren

Copyright © 2022 Taotao Hu et al. This is an open access article distributed under the Creative Commons Attribution License, which permits unrestricted use, distribution, and reproduction in any medium, provided the original work is properly cited.

The problem of tunnel lining cracking is becoming more and more common. The existence of cracks changes the stress state of lining structure and has an adverse impact on the safety of lining structure. In this paper, the mechanical properties of tunnel cracked lining structure are studied. Based on the theories of structural mechanics and fracture mechanics, the performance indexes of cracks in the arch waist of tunnel secondary lining are studied with the reference of stress intensity factor. The numerical simulation calculation is carried out. Finally, the XFEM extended finite element method is used, the crack damage of secondary lining under different crack depths is demonstrated and analyzed, and the theoretical value is compared with the numerical value. The results show that, for the cracked model (the crack depth is 12 cm), the stress and displacement at the arch waist increase greatly compared with the uncracked model and are the most significant with the increase of crack depth. In the initial stage of crack development, the growth of stress and displacement of the structure is not obvious, and the small change of crack depth in the later stage can also cause great growth of stress and displacement. Compared with the uncracked model, when the crack depth is 3 cm, the maximum vertical stress increases by 4.3 times and the maximum settlement increases by 1.3 times. When the crack depth is 18 cm, it increases by 21.2 times and 2.94 times, respectively. The research results can provide a theoretical basis for the prevention and treatment of cracks in the arch waist of tunnel secondary lining during tunnel operation.

1. Introduction

The number and scale of tunnels around the world are increasing, but various diseases and problems during tunnel operation also follow, among which the most common problem is the cracking of tunnel secondary lining. It is very important to study tunnel lining cracks. Fracture mechanics is a powerful tool to study cracks. It mainly studies the failure of materials and structures with defects. This paper will study the application of fracture mechanics theory in tunnel lining cracks.

Many scholars [1–5] published various views about the theory of fracture mechanics previously. Based on the development of fracture mechanics theory, some scholars [6–10] obtained the relevant physical and mechanical parameters of rock mass through experimental research, which provided a theoretical basis for the external force factors affecting the stress state of tunnel lining, and more and more scholars [11–15] pay attention to the influence of cracks on the safety of tunnel lining structure through model experiments and gradually improve the research system of the influence of cracks on materials and structures. Huang et al. [16] used extended finite element method to study the distribution law, propagation process, appearance, and occurrence mechanism of cracks in lining under the action of main influencing factors, providing a reference for the analysis of causes of cracks in lining. Li et al. [17] used the elastoplastic damage constitutive model of concrete to study the stress, damage, and bearing capacity of tunnel lining structure through simulation calculation and found that the

crack of the vault is mainly caused by the tension of the lining structure. Wang et al. [18] calculated the stress intensity factor of lining crack tip based on fracture mechanics theory and established a theoretical analysis method for crack stability of plain concrete lining of highway tunnel. Yu [19] discussed the influence of cracks on the safety of lining structures and found that when the structure was fractured in one part and could no longer bear the bending moment, its overall stress distribution would change, and larger bending moments would be generated in other parts, thus inducing new cracking. Yuan [20] adopted the research means of combining model test and numerical simulation, revealing that the existence of cracks would have an impact on the load, lining stress, and crack depth imposed on each part of the lining when cracking.

At the same time, many scholars pay attention to the influence of crack depth on the safety of tunnel lining structure. Xu [21] applied the theory of fracture mechanics to analyze the fracture behavior when longitudinal cracks were located in the tunnel vault and obtained the influence law of crack depth on the stress intensity factor. Liu et al. [22] analyzed the influence of crack location, crack depth, and formation resistance on the bearing capacity of lining structure and found that the safety factor of tunnel vault decreases linearly with the increase of crack depth, and under the condition of the same crack depth, the crack is the most unfavorable in the vault and has little impact on the structural safety factor in the arch waist, side wall, and arch foot. Zhang [23] applied finite element numerical analysis and found that crack depth had a significant impact on the safety of tunnel lining structure. Liu et al. [24] used finite element software to conduct numerical simulation analysis on the stress performance of tunnel lining cracks and found that the greater the crack depth, the greater the displacement and stress of tunnel structure, and the more obvious the stress concentration at the crack tip. Zheng [25] proposed that the crack depth should be used as a reference index for the classification of lining cracking diseases. Wang et al. [26] analyzed the impact of cracks of different lengths and depths on the safety of lining structure and found that the damage degree of arch crack to lining structure is much greater than that of arch waist crack, and crack depth has a more significant impact on the safety of lining structure than crack length. Through numerical simulation software, Liu and Han [27] found that when the lining vault cracks, the crack depth is positively correlated with the stress intensity at the crack tip and negatively correlated with the stability coefficient. Based on fracture mechanics and concrete fracture mechanics theory, Huang [28] obtained the variation rule of stress intensity factor and stability factor at various positions with crack depth and Angle. Yang et al. [29] studied the effects of crack location, crack depth, and crack width on the stress of lining structure. The results show that, with the change of crack depth and width, the position of the most dangerous section of tunnel lining also changes. Xiao et al. [30] used finite element software to establish finite element models of tunnel lining with different crack depths and fracture positions and found that the arch crack is the most harmful to the structure, and the crack depth has a significant impact on the bearing performance of the structure. Zhao et al. [31] calculated the stress intensity factor at the crack tip, indicating that the proportion and influence of longitudinal cracks in lining diseases are the largest, and the stability of lining cracks is closely related to crack location, crack type, and crack angle.

A large number of studies show that the factor of tunnel lining crack depth has a greater impact on structural safety, but there is a lack of clear research on lining crack with crack depth as a parameter. Therefore, based on the theory of linear elastic fracture mechanics, this paper establishes the calculation model of tunnel cracked lining structure with different crack positions and depths, compares it with the noncrack model, arranges and analyzes the calculation results, summarizes the relationship between crack depth and structural safety, and then establishes a research and analysis of tunnel lining cracking with crack depth as variable.

2. Study on Fracture Mechanics Theory of Tunnel Lining Structure

2.1. Numerical Simulation Model of Concrete Cracks. The fracture mechanics model mainly studies the crack propagation and instability of existing structures and considers the effect of crack tip stress concentration on crack propagation. This model can simulate the width, length, and depth of cracks, but only a single crack can be considered. This paper mainly studies the crack propagation of cracked lining structure and the residual bearing capacity after cracking. Therefore, the fracture mechanics model is used to deal with the cracks of the secondary lining structure in this numerical simulation analysis.

There are many types of cracks with combined characteristics in the actual tunnel structure, among which type I-II composite crack is the most common and dangerous crack form. The tunnel problem is simplified as a plane strain problem. It is assumed that the main cracking modes of the tunnel lining cracks are type I cracks and type I-II composite cracks. Therefore, this paper mainly studies the fracture mechanics theory of single open fracture (type I) [32].

2.2. Overview of the Tunnel Lining Structure. The authenticity of the numerical analysis results of tunnel secondary lining depends on whether the corresponding numerical model is reasonable or not. In order to better compare and analyze with the test data, this modeling only considers the secondary lining structure and studies the stress-strain at the crack tip and the bearing capacity of the structure. The thickness of the secondary lining of a tunnel is 40 cm, and an inverted arch is set. The section of the lining structure is shown in Figure 1.

2.3. Structural Mechanics Calculation of the Tunnel Lining Structure. In the tunnel structure, the longitudinal cracks have serious harm to the structure, and the arch waist of the lining structure is stressed greatly and there are many cracks. Therefore, this paper studies and analyzes the arch waist of the secondary lining. The tunnel adopts curved wall lining

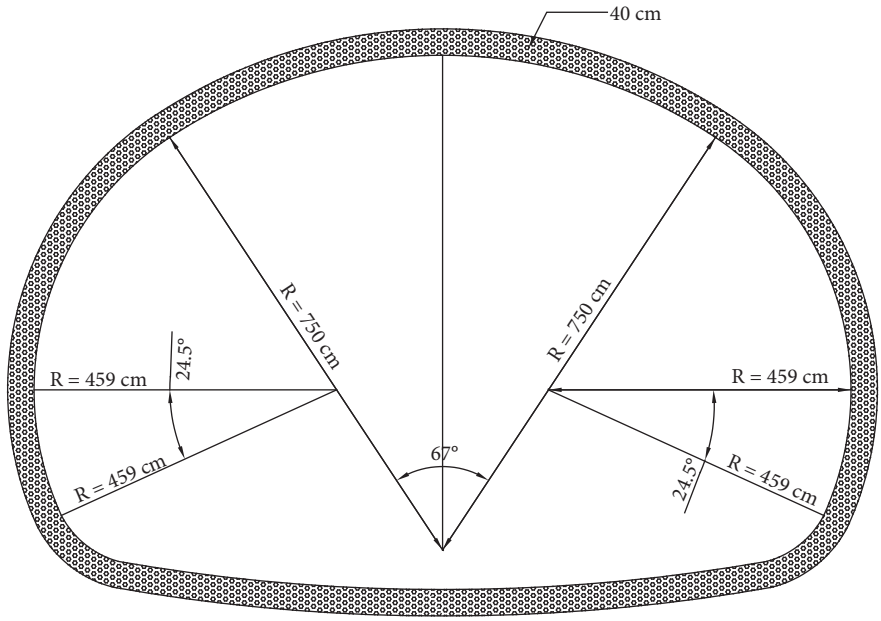

Figure 1: Section of secondary lining.

form, which is composed of arch ring, curved side wall, and bottom plate. When there is upward bottom pressure, inverted arch is set. The arch ring and curved side wall are calculated as a whole without hinged arch, and the influence of inverted arch on lining internal force is generally not considered [33].

2.3.1. Force Method Equation and Lining Internal Force under Active Load. The basic structure is shown in Figure 2. The unknown forces are X_{1p} and X_{2p}. According to the condition that the relative displacement of the arch waist section is zero, the force method equation can be listed:

$$\begin{aligned} X_{1P}\delta_{21} + X_{2P}\delta_{22} + \Delta_{2p} + f\beta_{ap} + u_{ap} = 0, \\ X_{1P}\delta_{11} + X_{2P}\delta_{12} + \Delta_{1p} + \beta_{ap} = 0, \end{aligned} \tag{1}$$

where β_{ap} and u_{ap} are the displacement of wall bottom. Calculate the effects of X1p, X2p, and external load, respectively, and then add them according to the superposition principle to obtain

$$\beta_{ap} = X_{1P}\overline{\beta}_1 + X_{2P}\left(\overline{\beta}_2 + f\overline{\beta}_1\right) + \beta_{ap}^0. \tag{2}$$

Since the horizontal displacement is not considered at the wall bottom, $u_{ap} = 0$, substitute (1) to obtain

$$\begin{aligned} X_{1P}\left(\delta_{21} + f\overline{\beta}_1\right) + X_{2P}\left(\delta_{22} + f^2\overline{\beta}_1\right) + \Delta_{2P} + f\beta_{ap}^0 = 0, \\ X_{1P}\left(\delta_{11} + \overline{\beta}_1\right) + X_{2P}\left(\delta_{12} + \overline{\beta}_2 + f\overline{\beta}_1\right) + \Delta_{1P} + \beta_{ap}^0 = 0, \end{aligned} \tag{3}$$

where δ_{ik} and Δ_{ip} are the element displacement and active load displacement of the basic structure; $\overline{\beta}_1$ is the unit rotation angle of the wall bottom (°); β_{ap}^0 is the load rotation angle of the wall bottom of the basic structure (°); f is the lining rise (m).

After calculating X1p and X2p, under the action of active load, the internal force of lining is

$$\begin{aligned} N_{ip} &= X_{2p} + X_{2p}\cos\varphi_i + N_{ip}^0, \\ M_{ip} &= X_{1p} + X_{2p}y_i + M_{ip}^0. \end{aligned} \tag{4}$$

2.3.2. Calculation of Final Internal Force of Lining. When the $\sigma_h = 1$ elastic resistance diagram is regarded as the external load acting alone, the excess force $X_{1\sigma}, X_{2\sigma}$ can be obtained by referring to the calculation method of X1p and X2p, and the output method equation is listed:

$$\begin{aligned} X_{1\sigma}\left(\delta_{21} + f\overline{\beta}_1\right) + X_{2\sigma}\left(\delta_{22} + f^2\overline{\beta}_1\right) + \Delta_{2\sigma} + f\beta_{a\sigma}^0 = 0, \\ X_{1\sigma}\left(\delta_{11} + \overline{\beta}_1\right) + X_{2\sigma}\left(\delta_{12} + f\overline{\beta}_1\right) + \Delta_{1\sigma} + \beta_{a\sigma}^0 = 0, \end{aligned} \tag{5}$$

where $\Delta_{1\sigma}, \Delta_{2\sigma}$ is the displacement of the basic structure in $X_{1\sigma}, X_{2\sigma}$ direction caused by the load in the unit elastic resistance diagram (m); $\beta_{a\sigma}^0$ is the rotation angle (°) of the wall bottom of the basic structure caused by the load in the unit elastic resistance diagram; $\beta_{a\sigma}^0 = M_{a\sigma}^0\overline{\beta}_1$. The meaning of other symbols is the same as above.

After solving $X_{1\sigma}, X_{2\sigma}$, the internal force of any section of lining under the single action of load in the unit elastic resistance diagram can be calculated:

$$\begin{aligned} N_{i\sigma} &= X_{2\sigma}\cos\varphi_i + N_{i\sigma}^0, \\ M_{i\sigma} &= X_{1\sigma} + X_{2\sigma}y_i + M_{i\sigma}^0. \end{aligned} \tag{6}$$

The final internal force value of any section of lining can be obtained by using the superposition principle:

$$\begin{aligned} N_i &= N_{ip} + \sigma_h N_{i\sigma}, \\ M_i &= M_{ip} + \sigma_i M_{i\sigma}. \end{aligned} \tag{7}$$

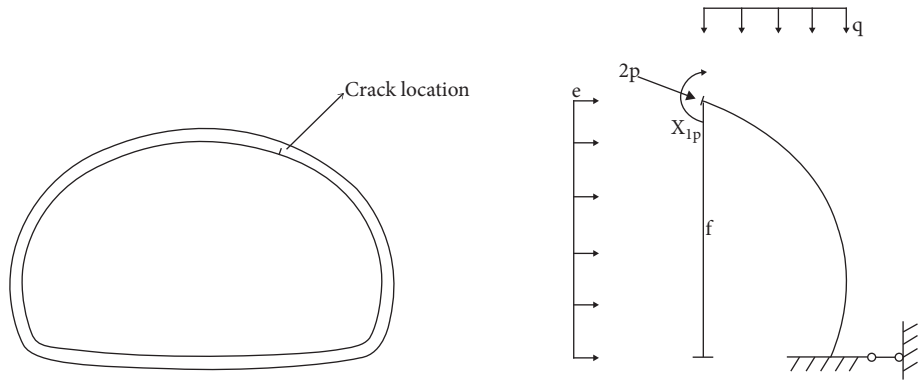

Figure 2: Basic structural stress diagram.

According to the above, the arch waist bending moment M_d and the arch waist axial force N_d can be finally obtained.

2.4. Fracture Mechanics Calculation of Tunnel Lining Structure. Most of the cracks in the tunnel lining structure are longitudinal cracks. The cracks in the arch waist of the longitudinal cracks do great harm to the lining structure. Therefore, this paper only analyzes the longitudinal cracks in the arch waist.

2.4.1. Fracture Mechanics Calculation Model. In this paper, the thickness of the secondary lining of the model is $h = 40$ cm. In order to analyze the crack at the arch waist more conveniently, the arch lining structure is approximately linear on the left and right sides of the center line. At present, the crack is mainly evaluated by the width of the crack. The wider the crack, the greater the harm to the structural safety. In the actual structure, the depth of crack plays an important role in the structure, and the width is considered to be the expression of depth. For the calculation model in this paper, in order to discuss the influence of different crack depths on the structure, the crack depth at the arch waist is determined as $a = 3$~18 cm. The arch waist bending moment M_d and arch crown axial force N_d of the structure can be obtained from Section 2.3. The final calculation model and crack simplified model are shown in Figure 3.

2.4.2. Calculation of Stress Intensity Factor. The calculation of the stress intensity factor of the model is divided into two parts; that is, the results are calculated under the separate action of the arch waist bending moment M_d and the arch waist axial force N_d. Then the stress intensity factor under the load of the model is obtained according to the superposition principle.

(1) Single Side Crack in Pure Bending [34]. The infinite strip with width b has a unilateral crack with depth "a," which acts on the bending moment M per unit thickness, as shown in Figure 4, and its stress intensity factor is

$$K_{IM} = F\sigma\sqrt{\pi a}, \tag{8}$$

where

$$F = \sqrt{\frac{2b}{\pi a} tg \frac{\pi a}{2b}}\ \frac{0.923 + 0.199\,(1 - \sin \pi a/2b)^4}{\cos \pi a/2b},$$
$$\sigma = \frac{6M}{b^2}. \tag{9}$$

Get

$$K_{IM} = S_M \cdot M, \tag{10}$$

where

$$S_M = F\frac{6}{b^2}\sqrt{\pi a}. \tag{11}$$

For the calculation model in this paper, when the secondary lining structure $B = 40$ cm, KIM is directly proportional to the arch waist bending moment M_d, while the bending coefficient SM is only related to the crack depth "a." When $a = 3$~18 cm, the values of F and S_M are obtained, as shown in Table 1.

It can be seen from Table 1 that when the crack depth "a" is small, the stress intensity factor changes slowly. When a is greater than 9 cm, the stress intensity factor increases rapidly, which also shows that when the crack depth reaches a certain value, the stress intensity factor mutates to reach the fracture toughness and fracture.

(2) Unilateral Crack Under Tension [34]. The infinite strip with width B has a unilateral crack with depth "a", which is subjected to unidirectional uniform tension, as shown in Figure 5, and its stress intensity factor is

$$K_{IN} = F\sigma\sqrt{\pi a}, \tag{12}$$

where

$$F = \sqrt{\frac{2b}{\pi a} tg \frac{\pi a}{2b}}\ \frac{0.752 + 2.02\,(a/b) + 0.37\,(1 - \sin \pi a/2b)^3}{\cos \pi a/2b},$$
$$\sigma = \frac{N}{A}. \tag{13}$$

Get

$$K_{IM} = S_N \cdot N, \tag{14}$$

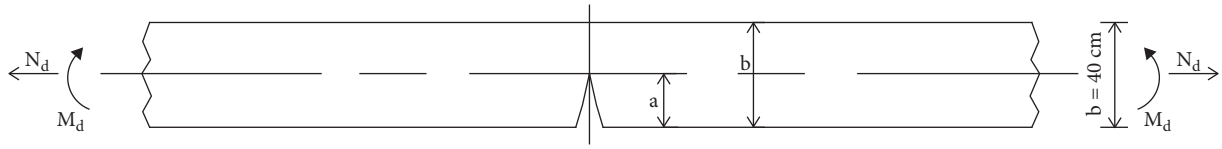

Figure 3: Fracture mechanics calculation model.

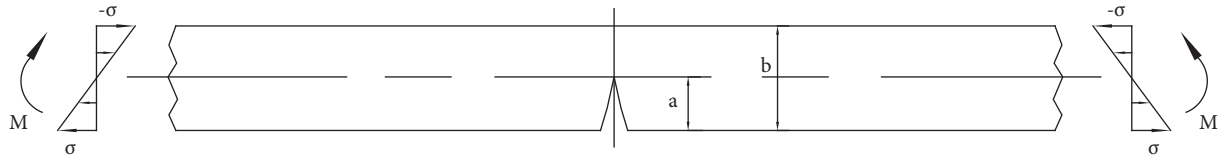

Figure 4: Pure bending calculation model.

Table 1: F and S_M values under pure bending.

Crack depth a (cm)	3	6	9	12	15	18
F	1.42	1.47	1.48	2.37	3.74	4.82
S_M ($m^{-3/2}$)	16.3	23.9	29.5	54.6	96.3	135.9

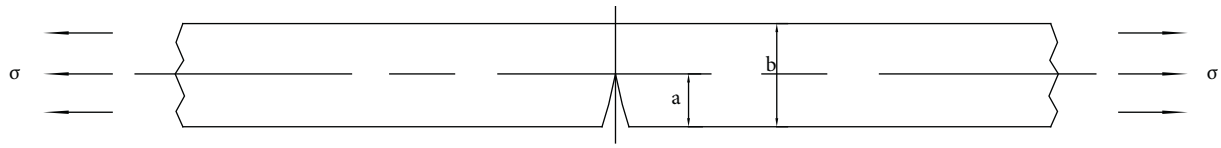

Figure 5: Pure tensile calculation model.

where

$$S_N = F\frac{\sqrt{\pi a}}{A}. \tag{15}$$

For the calculation model in this paper, when the secondary lining structure $B = 40$ cm, KIN is directly proportional to the arch waist bending moment M_d, while the tensile coefficient S_M is only related to the crack depth "a". When $a = 3$~18 cm, F and S_N values are obtained, as shown in Table 2.

It can be seen from Table 2 that when the crack depth "a" is small, the stress intensity factor changes slowly. When a is greater than 9 cm, the stress intensity factor increases rapidly, which also shows that when the crack depth reaches a certain value, the stress intensity factor mutates to reach the fracture toughness and fracture.

(3) Calculation of Stress Intensity Factor in Various Cases. In online elasticity, when several loads act on an elastomer at the same time, the stress and displacement caused by the load group at a certain point are equal to the sum of the stress and displacement components caused by each single load at that point. This is the superposition principle of linear elasticity theory [35]. Using this principle, when calculating K under complex load, it can also be decomposed into the sum of K under several simple load conditions.

According to the above superposition principle, the stress intensity factor under the joint action of arch waist bending moment M_d and arch waist axial force N_d is

Table 2: F and S_M values under pure tension.

Crack depth a (cm)	3	6	9	12	15	18
F	1.55	1.60	2.13	3.96	6.21	9.37
S_N ($m^{-3/2}$)	1.19	1.73	2.83	6.08	10.7	17.6

$$K_I = K_{IM} + K_{IN} = S_M \cdot M_d + S_N \cdot N_d. \tag{16}$$

When the arch waist bending moment M_d and the arch waist axial force N_d are constant, $b = 40$ cm, and "a" takes different values between 3 and 18 cm, the variation range of stress intensity factor K_I calculated from (12) is shown in Table 3.

It can be seen from Table 3 that, in the initial stage of crack development, the growth of stress intensity factor caused by the propagation of crack depth "a" is slow, but in the later stage, a small change in "a" leads to a huge change in stress intensity factor, which eventually leads to crack penetration and fracture.

3. Numerical Simulation of Tunnel Lining Cracks

3.1. Finite Element Model Establishment. The total length of the tunnel is 709 m, the geological condition is complex, the calculated section buried depth is 50 m, and the section surrounding rock is grade III. In the calculation, considering the symmetry of the structure, only the right half is taken to establish the model for analysis. The actual thickness of the

Table 3: Calculation results of stress intensity factor.

Crack depth a (cm)	K_I
$a = 3$	$16.3M_d + 1.19N_d$
$a = 6$	$23.9M_d + 1.73N_d$
$a = 9$	$29.5M_d + 2.83N_d$
$a = 12$	$44.6M_d + 6.08N_d$
$a = 15$	$67.3M_d + 10.7N_d$
$a = 16$	$93.3M_d + 12.8N_d$
$a = 17$	$117.2M_d + 14.7N_d$
$a = 18$	$135.9M_d + 17.6N_d$

Table 4: Physical and mechanical parameters of surrounding rock and support.

Material	Elastic modulus E (MPa)	Poisson's ratio	Bulk density (kN/m^3)	Cohesion (MPa)	Internal friction angle (°)	Dilatancy angle (°)
Surrounding rock (class IV)	2630	0.35	23	0.45	30	30
Shotcrete	21000	0.2	25	2	60	60
Secondary lining concrete	31000	0.2	25	3	60	60
Bolt	200000	0.3	78	—	—	—

soil layer above the top of the tunnel is 50 m, the left and right is 100 m, and below the tunnel is 100 m. The calculation boundary conditions are: horizontal constraint on the right, vertical constraint on the lower, and symmetrical constraint on the left.

According to "the code for design of highway tunnels [36]," the stress analysis of the tunnel should be analyzed according to the grade reduction of surrounding rock. Therefore, the section with a buried depth of 50 m of the tunnel should be calculated and analyzed according to grade IV surrounding rock. The yield condition of surrounding rock and concrete is Drucker–Prager criterion [37], and its physical and mechanical parameters are shown in Table 4.

The calculation model of surrounding rock and lining structure model are shown in Figures 6 and 7, respectively.

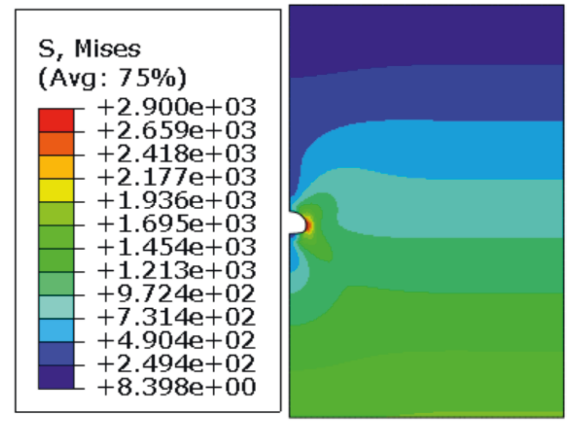

Figure 6: Calculation model of surrounding rock.

3.2. Analysis and Comparison of Cracked and Uncracked Models. In order to better analyze the displacement and stress of the crack model, the finite element calculation results of the lining structure in the uncracked model and the crack model (crack depth 12 cm) are compared in this paper, as shown in Table 5. The displacement diagrams and directional stress diagrams of the two models are shown in Figures 8–11.

It can be seen from the results in Table 5 that, for the cracked model, the displacement and stress at the lining arch waist are much higher than those of the uncracked model. It means that once longitudinal cracks appear in the lining, the safety of the structure will be greatly endangered. The maximum stress at the crack occurs at the crack tip; that is, the crack tip is a dangerous point. The research on crack body under plane stress state shows that [38], for type I crack, when the lining concrete material meets $K_c \geq K_c$ or $\delta \geq \delta_c$, the model will fail and the crack begins to expand.

3.3. Analysis and Comparison between Models with Different Values of Crack Depth. Under the same load conditions, when the size parameters of the model are different, the stress intensity factor KI of the lining structure is also different. The crack depth "a" at the arch waist is 3 cm, 6 cm, 9 cm, and 18 cm, respectively, for calculation. The calculated stress intensity factor KI, vertical maximum stress, and maximum settlement are listed in Table 6.

The stress and displacement nephogram in Y-direction is shown in Figures 12–19.

Through the comparison of data in Table 6 and Figures 12–19, it can be seen that, at the crack tip, the greater the crack depth "a," the greater the stress intensity factor, the increase trend of vertical maximum stress and maximum settlement at the arch waist, the more obvious the stress concentration at the crack tip, and the final stress intensity factor increases to the fracture toughness, resulting in fracture and structural damage.

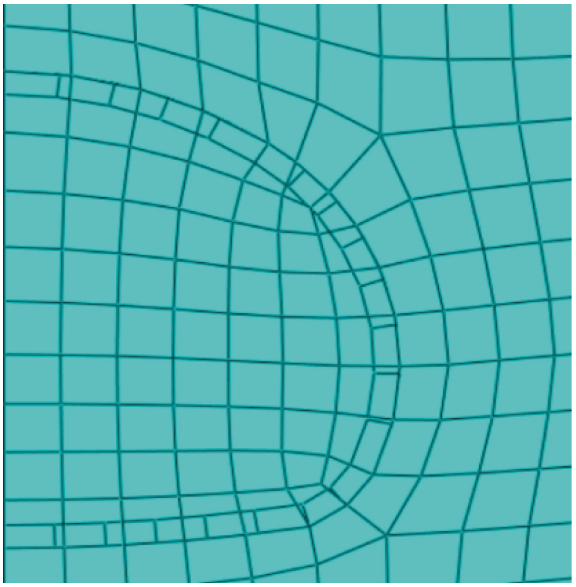

Figure 7: Lining structure model and unit division.

Table 5: Comparison of calculation results of finite element model.

	Uncracked model	Cracking model
Maximum settlement of lining arch waist (mm)	10.96	23.12
Maximum vertical stress of lining arch waist (MPa)	17.04	174.4

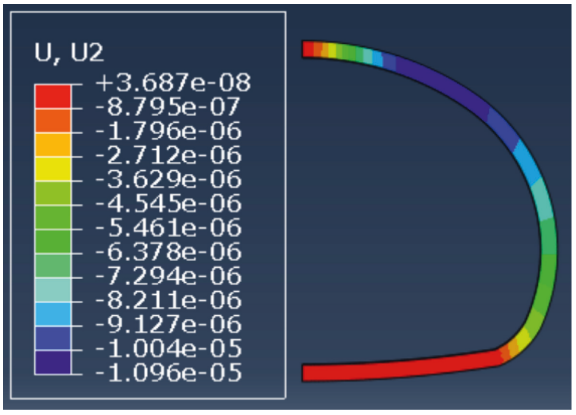

Figure 8: *Y*-direction displacement diagram.

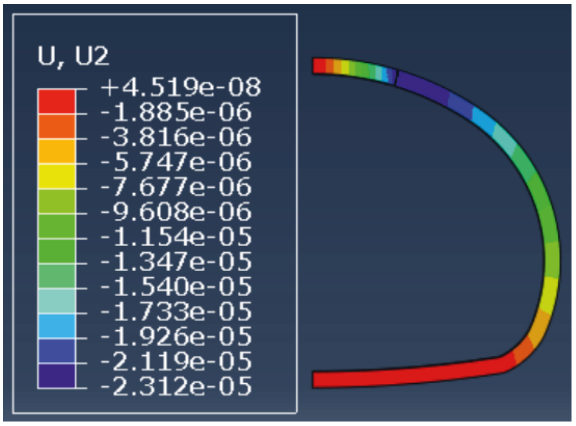

Figure 9: *Y*-direction displacement diagram of uncracked model of cracking model.

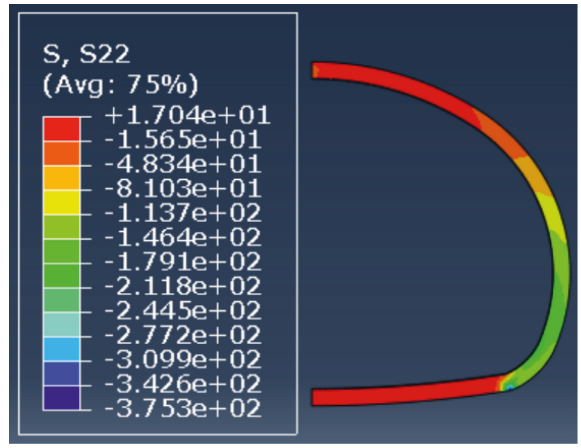

Figure 10: Y-direction stress diagram of uncracked model.

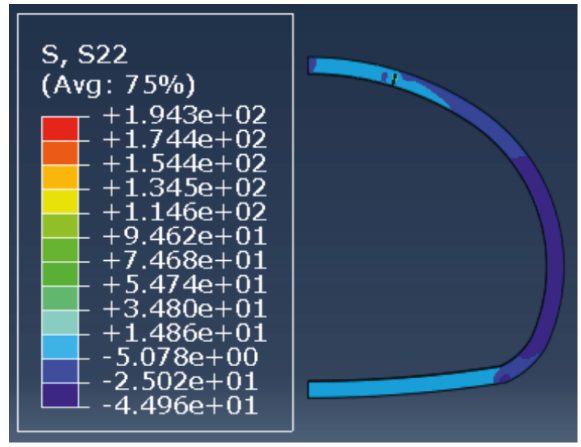

Figure 11: Y-direction stress diagram of cracking model.

Table 6: K_I values under different crack depths.

Crack depth a (cm)	a/h	Stress intensity factor KI	Maximum vertical stress (MPa)	Maximum settlement (mm)
3	0.075	0.35	74.37	14.21
6	0.15	0.77	123.8	18.41
9	0.225	1.14	152.6	20.20
18	0.45	5.35	362.2	32.21

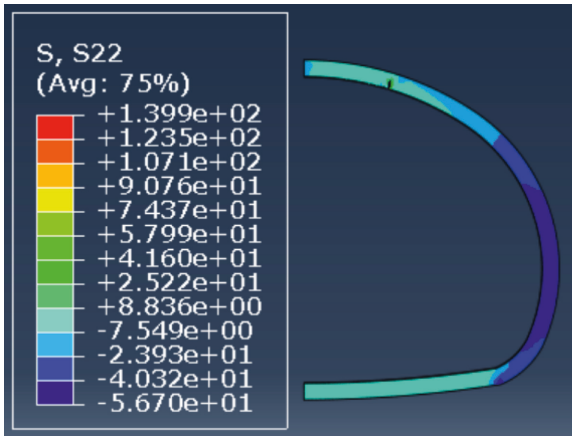

Figure 12: Y-direction stress diagram of $a = 3$ cm model.

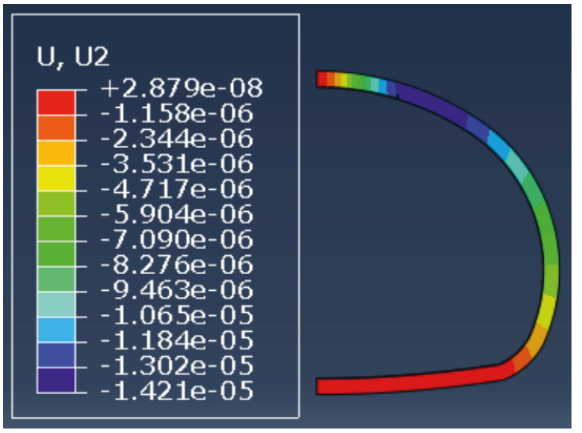

Figure 13: Y-direction displacement diagram of $a = 3$ cm model.

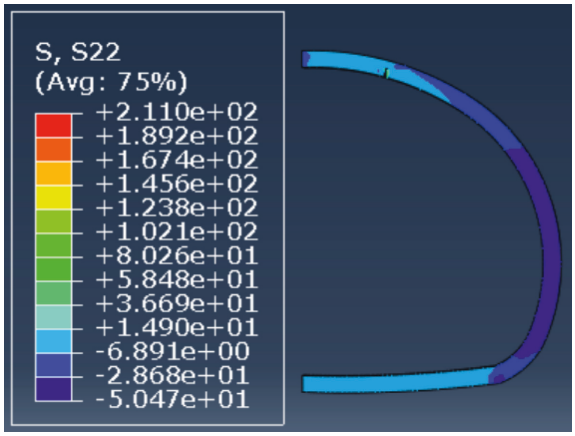

Figure 14: Y-direction stress diagram of $a = 6$ cm model.

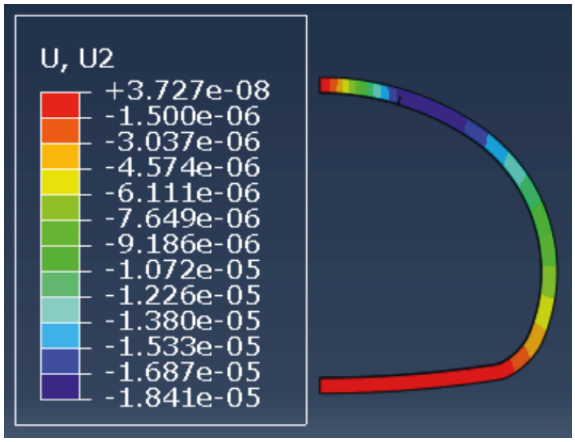

Figure 15: Y-direction displacement diagram of $a = 6$ cm model.

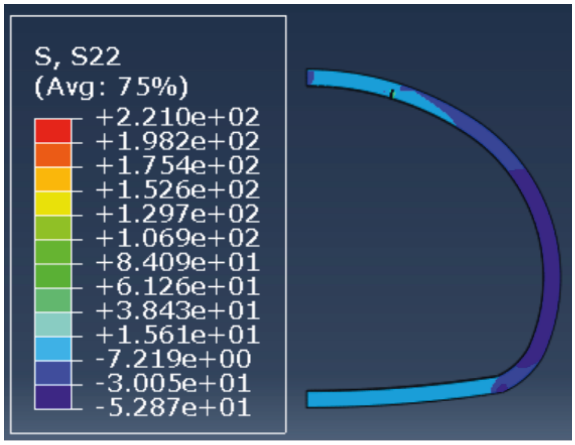

Figure 16: Y-direction stress diagram of $a = 9$ cm model.

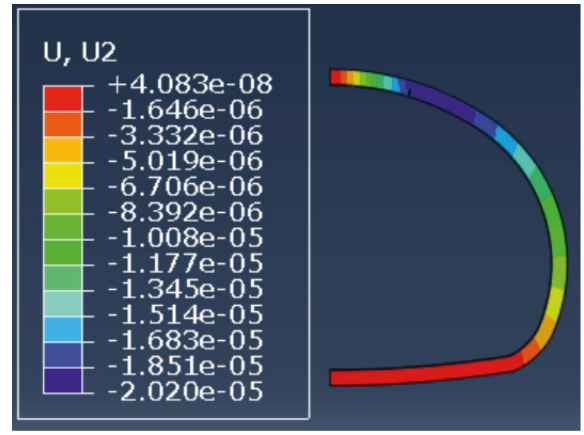

Figure 17: Y-direction displacement diagram of $a = 9$ cm model.

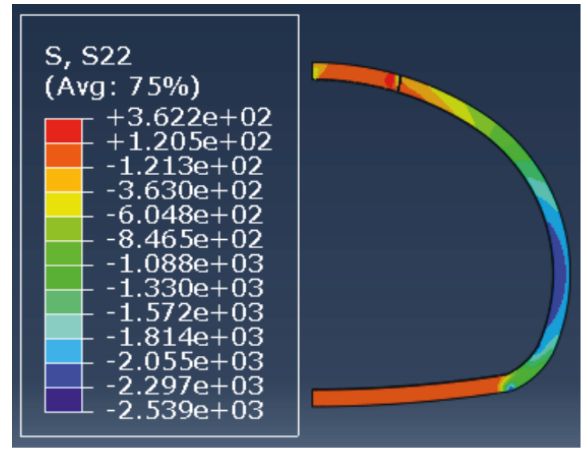

Figure 18: Y-direction stress diagram of $a = 18$ cm model.

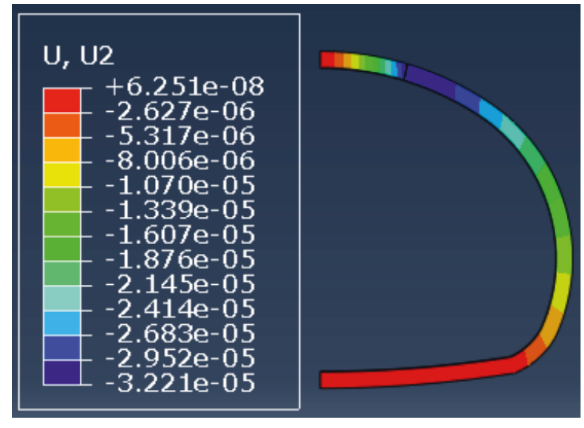

Figure 19: Y-direction displacement diagram of $a = 18$ cm model.

4. Comparison between Theoretical Value and Numerical Value

The stress intensity factor KI of the secondary lining calculation model is calculated according to Table 3, and compared with the numerical value, the detailed results are shown in Table 7, and the comparison curve is shown in Figure 20.

It can be seen from Table 7 and Figure 20 that the difference between the theoretical value and the numerical value is about 10%. Considering the coarse mesh division in the model in this paper, some calculation parameters need to be discussed. In order to make the calculation results more accurate, more mesh seeds can be arranged near the crack position and reduce the mesh size. It is believed that, with the

Table 7: Comparison between K_I theoretical value and numerical calculation results.

Crack depth a (cm)	K_I numerical value (MPa·m$^{1/2}$)	K_I theoretical calculated value (MPa·m$^{1/2}$)	Error (%)
3	0.35	0.31	−11.43
6	0.77	0.85	10.39
9	1.14	1.25	9.65
12	2.13	2.04	−4.23
15	3.51	3.31	−5.70
18	5.35	4.93	−7.85

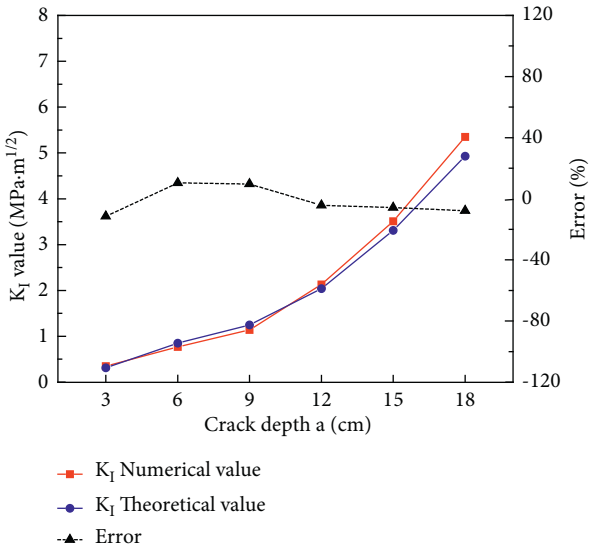

Figure 20: Comparison curve of KI theoretical value and calculated value.

more and more precision of the mesh and the optimization of the finite element model, the numerical calculation results will be closer to the theoretical value.

5. Conclusion

Tunnel lining cracks seriously affect the safe construction and operation of tunnel structure. With the development of fracture mechanics and its wide application in concrete, this paper mainly uses the theory of fracture mechanics to analyze the crack problem of tunnel structure. Through numerical calculation and theoretical analysis, the application of fracture mechanics in tunnel lining cracking is studied, and the following conclusions are obtained.

(1) The fracture mechanics model is used to simulate and analyze the cracking of the secondary lining structure, and the longitudinal cracks in the arch waist of the secondary lining are analyzed by fracture mechanics. The calculation of structural mechanics and fracture mechanics of lining structure shows that, in the early stage of crack development, the propagation of crack depth has little effect on the growth of stress intensity factor, but in the later stage, the small change of crack depth will have a great impact on stress intensity factor and eventually lead to crack penetration and fracture.

(2) The stress and displacement at the arch waist of uncracked model and cracked model are analyzed by ABAQUS finite element analysis software. For the cracked model, the displacement and stress at the arch waist of the lining are much higher than those of the uncracked model. This means that once longitudinal cracks appear in the lining, the safety of the structure will be greatly endangered.

(3) By analyzing and comparing the stress intensity factor, vertical maximum stress and maximum settlement between different crack depth models, it shows that, at the crack tip, the greater the crack depth, the greater the stress intensity factor, the increase trend of vertical maximum stress and maximum settlement at the arch waist, and the more obvious the stress concentration at the crack tip. Finally, the stress intensity factor increases to the fracture toughness, resulting in the failure of the structure.

Data Availability

The data in this paper are obtained according to theoretical derivation and numerical simulation. The subject needs further research and is inconvenient to be disclosed. The data that support the findings of this study are available from the corresponding author upon reasonable request.

Conflicts of Interest

The authors declare that they have no conflicts of interest.

Acknowledgments

This research was supported by National Key R&D Program of China (Grant Number: 2018YFB1600100), National Natural Science Foundation of China (Grant no. 51908052), Natural Science Basic Research Program of Shaanxi (Program nos. 2022JM-203, 2020JQ-371), the Open Fund of State Key Laboratory for Strength and Vibration of Mechanical Structures (Grant No. SV2019-KF-13), and Xi'an Jiaotong University.

References

[1] J. W. Hutchinson, "Singular behaviour at the end of a tensile crack in a hardening material," *Journal of the Mechanics and Physics of Solids*, vol. 16, no. 1, pp. 13–31, 1968.

[2] J. R. Rice and G. F. Rosengren, "Plane strain deformation near a crack tip in a power-law hardening material," *Journal of the Mechanics and Physics of Solids*, vol. 16, no. 1, pp. 1–12, 1968.

[3] J. W. Hutchinson and P. C. Paris, *Stability Analysis of J-Controlled Crack Growth*, pp. 37–61, ASTM STP 668 Philadelphia. Ame. Soc. Testing & . Mater, 1979.

[4] C. Zhu, M. Karakus, M. C. He et al., "Volumetric deformation and damage evolution of Tibet interbedded skarn under multistage constant-amplitude-cyclic loading," *International Journal of Rock Mechanics and Mining Sciences*, vol. 152, 2022.

[5] Y. Wang, H. N. Yang, J. Q. Han, and C. Zhu, "Effect of rock bridge length on fracture and damage modelling in granite containing hole and fissures under cyclic uniaxial increasing-amplitude decreasing-frequency (CUIADF) loads," *International Journal of Fatigue*, vol. 158, 2022.

[6] Z.-j. Wu, Z.-y. Wang, L.-f. Fan, L. Weng, and Q.-s. Liu, "Micro-failure process and failure mechanism of brittle rock under uniaxial compression using continuous real-time wave velocity measurement," *Journal of Central South University*, vol. 28, no. 2, pp. 556–571, 2021.

[7] X. S. Li, Q. H. Li, and Y. J. Hu, "Study on three-dimensional dynamic stability of open-pit high slope under blasting vibration," *Lithosphere*, vol. 2022, Article ID 6426550, 2022.

[8] H. Peijie, *Study on Type I Fracture Characteristics of Granite under Cyclic Loading and Unloading*, Shandong University of architecture, Jinan, China, 2020.

[9] C. Zhu, M. C. He, X. H. Zhang, Z. G. Tao, Q. Yin, and L. F. Li, "Nonlinear mechanical model of constant resistance and large deformation bolt and influence parameters analysis of constant resistance behavior," *Rock and Soil Mechanics*, vol. 42, no. 7, pp. 1911–1924, 2021.

[10] Qi. Wang, S. Xu, M. He, B. Jiang, W. Huayong, and Y. Wang, "Dynamic mechanical characteristics and application of constant resistance energy-absorbing supporting material," *International Journal of Mining Science and Technology*, vol. 19, 2022.

[11] Q. Wang, M. He, S. Li et al., "Comparative study of model tests on automatically formed roadway and gob-side entry driving in deep coal mines," *International Journal of Mining Science and Technology*, vol. 31, no. 4, pp. 591–601, 2021.

[12] Y.-q. Su, F.-q. Gong, S. Luo, and Z.-x. Liu, "Experimental study on energy storage and dissipation characteristics of granite under two-dimensional compression with constant confining pressure," *Journal of Central South University*, vol. 28, no. 3, pp. 848–865, 2021.

[13] Z. Dou, S. X. Tang, X. Y. Zhang et al., "Influence of shear displacement on fluid flow and solute transport in a 3D rough fracture," *Lithosphere*, vol. 4, 2021.

[14] P. Zhang, D. F. Zhang, Y. Yang et al., "A case study on intergrated modeling of spatial information of a complex geological body," *Lithosphere*, vol. s10, 2022.

[15] L. Liu, Z. Li, G. Cai, X. Geng, and B. Dai, "Performance and prediction of long-term settlement in road embankments constructed with recycled construction and demolition waste," *Acta Geotechnica*, vol. 256, 2022.

[16] H. Huang, D. Liu, Y. Xue, P. Wang, and L. Yin, "Numerical analysis of tunnel lining crack cracking based on extended finite element," *Journal of geotechnical engineering*, vol. 35, no. 2, pp. 266–275, 2013.

[17] Y. Li, M. Wang, H. Xu, Y. Zhang, and D. Wang, "Stress analysis of subway tunnel lining structure with crack disease," *China Railway Science*, vol. 35, no. 3, pp. 64–69, 2014.

[18] Y. Wang, Z. Liu, S. Zhang, J. Qiu, and Y. Xie, "Crack stability analysis of plain concrete lining of in-service highway tunnel," *Chinese Journal of highway*, vol. 28, no. 7, pp. 77–85, 2015.

[19] J. Yu, "Study on the influence law of highway tunnel lining cracks on structural stress distribution," *Journal of Civil Engineering*, vol. 50, no. S1, pp. 70–75, 2017.

[20] T. Yuan, *Study on the Influence of Tunnel Lining Cracking on Structural Mechanical Performance*, Beijing Jiaotong University, Beijing, China, 2019.

[21] M. Xu, *Application of Fracture Mechanics Theory in Highway Tunnel Lining Cracking*, Chongqing Jiaotong University, Chongqing, China, 2008.

[22] X. Liu, P. Zhang, and M. Zhou, "Analysis of the influence of longitudinal cracks on the bearing capacity of tunnel lining," *Journal of rock mechanics and engineering*, vol. 31, no. 10, pp. 2096–2102, 2012.

[23] Y. Zhang, *Safety Evaluation of Damaged Tunnel Structure Based on Finite Element Method*, Lanzhou Jiaotong University, Anning, China, 2013.

[24] F. Liu, L. Liu, and B. C. A. I. Wang, "Influence analysis of lining cracks on tunnel stability," *Journal of Shijiazhuang Railway University (NATURAL SCIENCE EDITION)*, vol. 26, no. S2, pp. 180–182+187, 2013.

[25] Y. Zheng, *Study on Lining Crack Mechanism and Structural Safety Evaluation of Highway Tunnel*, Central South University, Hunan, China, 2014.

[26] W. Wang, J. Deng, and J. Yin, "Study on safety of railway tunnel lining structure under space crack disease," *China Science and technology of work safety*, vol. 12, no. 1, pp. 33–37, 2016.

[27] Y. Liu and Y. Han, "Classification of tunnel lining cracking disease based on fracture mechanics theory," *China Railway Science*, vol. 40, no. 3, pp. 72–79, 2019.

[28] R. Huang, *Study on Crack Stability of Highway Tunnel Based on Fracture Mechanics*, Chongqing Jiaotong University, Chongqing, China, 2020.

[29] Z. Yang, Z. Zhou, T. Ling, W. Wu, and J. Chen, "Study on the influence law of tunnel lining cracks on structural stress," *Traffic science and engineering*, vol. 36, no. 4, pp. 43–53, 2020.

[30] S. Xiao, Ke. Li, X. Jiang, S. Wu, and C. Yao, "Study on bearing safety and crack evaluation standard of cracked lining," *Highway traffic technology*, vol. 37, no. S1, pp. 41–47, 2021.

[31] W. Zhao, R. Huang, bin. Zeng, N. Peng, and H. Kou, "Multi factor analysis of lining crack stability of highway tunnel," *Journal of underground space and engineering*, vol. 17, no. S1, pp. 419–425, 2021.

[32] X. Yu, *Fracture Mechanics of Rock and concrete*, Central South University Press, Changsha, China, 1991.

[33] Z. Li and Y. Zhang, "Bearing capacity analysis and treatment technology of cracked tunnel," *Tunnel construction*, vol. 23, no. 4, 2003.

[34] China Academy of Aeronautics, *Manual of Stress Intensity Factors*, pp. 119-120, Science Press, Beijing, China, 2003.

[35] C. Jin and S. Zhao, *Fracture Mechanics*, Science Press, Beijing, China, 2006.

[36] JTG D70-2004, *Code for Design of Highway Tunnel*, 2004.

[37] Z. Xia, *Plastic Mechanics*, Tongji University Press, Shanghai, China, 1991.

[38] A. A. Wells, "Application of fracture mechanics of and beyond general yielding," *British Welding Journal*, vol. 10, pp. 563–570, 1963.